three axes of the low-temperature phase there is an antiferroelectric stacking of ferroelectric planes.

At 424 K, $[N(CH_3)_4][GeCl_3]$ undergoes a structural phase transition to the cubic phase with $a = 6\cdot552$ (2) Å. The heat of transformation is quite high with a value of $3\cdot1$ kJ mol⁻¹ (Möller, Wildermuth & Felsche, 1980). It should be noted that the range of thermal stability of the cubic phase is quite narrow. The compound decomposes 22 K above the transition point.

On approaching the transition temperature the ionic conductivity increases by several orders of magnitude. At the moment no mechanism can unambiguously be found for this effect. However, our model suggests possible paths of movement for the Cl atoms. The cubic lattice constant of $6\cdot552$ Å does not allow for a bonded Cl atom midway between two Ge atoms, since $3\cdot274$ Å is too long for a Ge—Cl bond. Therefore, we assume that this is a mean value for two Cl positions, each being approximately $2\cdot3$ Å from a Ge atom. The two Cl positions are separated by a potential barrier. This should not be too high, thus allowing a jumping of the Cl atom from one position to the other. This movement may be combined with a rotation of a $GeCl_3^-$ unit as a whole about a cubic axis, [100] or [111]. As a consequence two or three Cl atoms change axes. A combination of both mechanisms could explain the transport of chlorine. Further research is necessary to find the real mechanism. In this respect it is interesting to note that for the high-temperature phase of $Cs[GeCl_3]$ a type of disorder of the Cl atoms has been found which is in accordance with a double-well model. Furthermore, there is apparently some residual electron density midway between the Cl positions on the x and y axes (Fig. 4 of Christensen & Rasmussen, 1965).

References

BÄRNIGHAUSEN, H. (1975). *Acta Cryst.* A**31**, S3.
CHRISTENSEN, A. N. & RASMUSSEN, S. E. (1965). *Acta Chem. Scand.* **19**, 421–428.
FREGERSLEV, S. & RASMUSSEN, S. E. (1968). *Acta Chem. Scand.* **22**, 2541–2556.
GERMAIN, G., MAIN, P. & WOOLFSON, M. M. (1970). *Acta Cryst.* B**26**, 274–284.
GLAZER, A. M. (1972). *Acta Cryst.* B**28**, 3384–3392.
GLAZER, A. M. (1975). *Acta Cryst.* A**31**, 756–762.
International Tables for X-ray Crystallography (1974). Vol. IV, pp. 99, 149. Birmingham: Kynoch Press.
JOHNSON, C. K. (1965). *ORTEP.* Report ORNL-3794, revised. Oak Ridge National Laboratory, Tennessee.
MESSER, D. (1978). *Z. Naturforsch. Teil B*, **33**, 366–369.
MÖLLER, A. (1978). Annual Meeting of the German Physical Society, Freudenstadt, März.
MÖLLER, A. & FELSCHE, J. (1979). *J. Appl. Cryst.* **12**, 76–77.
MÖLLER, A., WILDERMUTH, G. & FELSCHE, J. (1980). To be published.

Solid–Solid Phase Transitions in $[NH(CH_3)_3]CdCl_3$

By Gervais Chapuis and F. Javier Zuniga

Institut de Cristallographie, Université de Lausanne, BSP, 1015 Lausanne, Switzerland

Abstract

Three phases of $[NH(CH_3)_3]CdCl_3$ (TrMCd) have been identified by X-ray diffraction in the temperature range 174 to 415 K. The low-temperature phase is orthorhombic, space group *Pbnm*, with $a = 8\cdot957$ (2), $b = 14\cdot348$ (4) and $c = 6\cdot6873$ (9) Å at 174 K; $Z = 4$. The structure was solved from single-crystal intensities and refined to $R = 0\cdot019$ including isotropically vibrating H atoms. The structure consists of one-dimensional chains of face-sharing $CdCl_6$ octahedra stacked perpendicularly to a nearly hexagonal net. The trimethylammonium ion is located in the free space between the chains and linked to a Cl atom by a hydrogen bond. The phase formed above 342 K is hexagonal, space group $P6_3/m$, $a_{h1} = 26\cdot049$ (5) and $c_{h1} = 6\cdot756$ (1) Å; $Z = 18$. Another hexagonal phase, space group $P6_3/m$, becomes stable in the temperature range 374 to 415 K with lattice constants $a_{h2} = 15\cdot06$ (2) and $c_{h2} = 6\cdot74$ (2) Å; $Z = 6$. Above 415 K, the compound decomposes in the solid state in two steps. The products, $[NH(CH_3)_3]Cd_3Cl_7$ and $CdCl_2$ respectively, have been identified by chemical analysis and powder diffraction. The dynamical behavior of the hydrogen-bonded trimethylammonium ion is responsible for the mechanism of the phase transitions.

1. Introduction

The recent development of the physics of low-dimensional solids has induced the search for and study of new materials with properties of reduced dimensions. Trimethylammonium cadmium chloride (TrMCd) belongs to this family and its structure is comparable to that of another one-dimensional solid, namely [N(CH$_3$)$_4$]MnCl$_3$ (TMMC) (Morosin & Graeber, 1967). In these materials, the metal atoms are located at the centers of face-sharing CdCl$_6$ octahedra forming infinite one-dimensional chains perpendicular to a hexagonal or nearly hexagonal net. The interchain distances are determined by the size of the organic cation which occupies the space between the octahedra. In TMMC and TrMCd, the distance between metal atoms of different chains is longer than the metal–metal distance within a chain by a factor of nearly three. This property is responsible for the one-dimensional physical properties of these materials and, in particular, for their magnetic characteristics (see, for example, Birgeneau & Shirane, 1978), which have been studied extensively both theoretically and experimentally for TMMC. The structure of TrMCd differs from that of TMMC owing to the presence of a hydrogen bond between the alkylammonium ion and a Cl atom. This bond is responsible for the low symmetry of the room-temperature phase as compared to the hexagonal symmetry of TMMC and also for the numerous solid–solid phase transitions existing up to a temperature of 415 K. In this article, we describe the structure of the low-symmetry phase of TrMCd and propose a model for the transition mechanism of the two high-temperature phases on the basis of powder and single-crystal X-ray diffraction measurements.
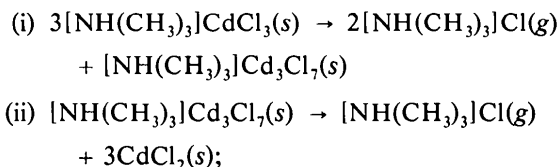
2. Experimental

The synthesis of TrMCd has been described elsewhere (Walther, Brinkmann, Chapuis & Arend, 1978). Suitable crystals for X-ray diffraction were obtained by slow evaporation from an aqueous solution. DTA data in the range 110 to 420 K show three sharp peaks at 342 $\pm$ 2, 374 $\pm$ 2 and 415 $\pm$ 2 K on a first heating cycle. Two additional effects of a much smaller amplitude could also be observed at 252 and 333 K. Additional heating cycles indicate the existence of an irreversible process when the sample is heated above 374 K.

2.1. *Identification of the phases*

A powder sample of TrMCd was analyzed on a Guinier chamber in the temperature range 295 to 450 K. An orthorhombic room-temperature phase (ORT) is uniquely observed up to 342 K. The lattice constants at 295 K are $a_o = 8 \cdot 986$ (3), $b_o = 14 \cdot 502$ (3) and $c_o = 6 \cdot 710$ (1) Å; $Z = 4$. Above 342 K, a new phase appears which is stable up to 374 K. This first high-temperature phase has hexagonal symmetry (HHT1) with the lattice parameters $a_{h1} = 26 \cdot 049$ (5) and $c_{h1} = 6 \cdot 756$ (1) Å; $Z = 18$. A second hexagonal high-temperature phase (HHT2) becomes stable in the temperature range 374 to 415 K with the lattice constants $a_{h2} = 15 \cdot 06$ (2) and $c_{h2} = 6 \cdot 74$ (2) Å; $Z = 6$. A drastic change in the powder diffractogram is observed above 415 K. The transition at this temperature is of the reconstructive type and is associated with a change of the stoichiometry of the material. This phase is stable up to 441 K. Above this temperature, we observe only the characteristic lines of CdCl$_2$ (space group $R\bar{3}m$).

To obtain a pure sample of the phase existing in the range 415 to 441 K, TrMCd was heated and maintained at 435 K for 48 h. After cooling, a powder diffractogram showed that this phase was also stable at room temperature. The chemical analysis of this sample revealed the existence of a new compound with the probable chemical formula [NH(CH$_3$)$_3$]Cd$_3$Cl$_7$ (TrCd$_3$Cl$_7$). Thus the transition of TrMCd to CdCl$_2$ is a two-step process resulting from the successive elimination of [NH(CH$_3$)$_3$]Cl as a gas according to the reactions

(i) $3[NH(CH_3)_3]CdCl_3(s) \rightarrow 2[NH(CH_3)_3]Cl(g)$

     $+ [NH(CH_3)_3]Cd_3Cl_7(s)$

(ii) $[NH(CH_3)_3]Cd_3Cl_7(s) \rightarrow [NH(CH_3)_3]Cl(g)$

     $+ 3CdCl_2(s);$

step (i) takes place above the temperature 415 $\pm$ 15 K whereas step (ii) is activated above 441 K.

All the phases described above coexist over a wide range of temperatures. At increasing temperatures, the characteristic lines of the ORT phase, for example, could still be observed at up to 30 K above the reported transition temperature; the same coexistence of two phases could also be observed in the temperature range 400 to 430 K showing that the transition of the HHT2 to TrCd$_3$Cl$_7$ is a very slow process with a large premonitory region. The transition of ORT–HHT1 is reversible whereas the transition HHT1–HHT2 already seems to be affected by the slow decomposition process.

The symmetries of the hexagonal phases have also been confirmed by single-crystal diffraction at temperatures within their domain of existence. To slow down the reconstructive process, the single crystal of the HHT2 phase was embedded in silicon grease.

2.2. *The structure of TrMCd at 174 K*

A transparent specimen of TrMCd with a prismatic habit elongated along **c** and dimensions 0·13 $\times$ 0·09 $\times$

0·20 mm was mounted on an automatic four-circle diffractometer (Syntex $P2_1$). The X-ray diffraction intensities were measured with Nb-filtered Mo $K\alpha$ radiation (λ_{Mo} = 0·71069 Å). The crystal was maintained at constant temperature within a few degrees by an open flow of cold nitrogen gas. This stream was surrounded by an additional stream of nitrogen gas at room temperature to prevent the formation of ice. The space group $Pbnm$ (standard $Pnma$, No. 62) was determined from the observed systematic absences and the results of the statistics based on the E values. With Z = 4 and the lattice constants at 295 K reported above, the calculated density D_{calc} = 2·119 (3) Mg m^{-3} is in good agreement with the density measured by flotation in a solution of CCl_4 and $CHBr_3$, D_m = 2·12 (1) Mg m^{-3}. Lattice constants at 174 K, a = 8·957 (2), b = 14·348 (4) and c = 6·6873 (9) Å, were calculated from the setting angles of 21 accurately centered reflections with 2θ values between 35 and 40°. Intensities up to (sin $\theta/\lambda)_{max}$ = 0·68 Å^{-1} with indices $\pm h,+k,+l$ were measured by the θ–2θ scan technique with an intensity-dependent scan speed varying between 2 and 10° min^{-1}. The background was evaluated by analyzing the scan profile (Schwarzenbach, 1977). The standard deviations of the intensities were obtained from counting statistics.

The stability of the measurements was checked periodically using three standard reflections; no significant variation could be observed during the experiment. The intensities were corrected for absorption (μ_{Mo} = 3·36 mm^{-1}) by the Gaussian integration method; the transmission coefficients varied between 0·661 and 0·784. The averaging of the data yielded 1243 independent observations, of which 988 had intensities larger than $3\sigma(I)$.

The program system XRAY 72 (Stewart, Kruger, Ammon, Dickinson & Hall, 1972; modified by D. Schwarzenbach) was used for the reduction of the data and the solution of the structure. Atomic scattering factors calculated by Cromer & Mann (1968) were assigned to Cd^{2+}, Cl^-, N^0 and C^0, whereas for H atoms

the values given by Stewart, Davidson & Simpson (1965) were used. Anomalous-scattering coefficients for Cd and Cl (Cromer & Liberman, 1970) have been included in the structure factor calculation.

The structure was solved from the Patterson synthesis. The nonhydrogen atoms were refined by full-matrix least squares with anisotropic thermal parameters. A difference Fourier synthesis revealed all the H atoms, which were subsequently included in the refinement with isotropic thermal parameters. The final residuals based on F values were R = 0·019 and R_w = $(\sum w|\Delta F|^2/\sum wF^2)^{1/2}$ = 0·019 with w = $1/\sigma^2(F)$; the goodness of fit $[\sum w\Delta F^2/(n - m)]^{1/2}$ was 1·96. The function minimized in the least-squares refinement was $\sum w\Delta F^2$. A final difference Fourier synthesis showed no peaks larger than 0·5 e Å^{-3} with the exception of one maximum at 0·85 e Å^{-3} at (0·41,0·13,0·25) (see below).* The atomic parameters of TrMCd at 174 K are reported in Table 1.

2.3. Description and discussion of the structure at 174 K

A projection of TrMCd along c showing the $CdCl_6$ octahedra is shown in Fig. 1. The Cd atoms lie at centers of symmetry whereas the Cl atoms and the trimethylammonium ions occupy the mirror plane perpendicular to c. As can be seen from the bond angles given in Table 2, the octahedra are elongated in the direction of a pseudo threefold axis parallel to c. The three independent Cl—Cd—Cl angles are approximately 84°, and thus differ considerably from the ideal angle of 90°. The three inequivalent Cd—Cl distances vary by 0·06 Å, the longest being due to the formation of a hydrogen bond bridging the N and Cl(2) atoms. The N—Cl(2) distance of 3·23 Å is comparable to the smallest N—H···Cl distances found in compounds of

---

* Lists of structure factors and thermal parameters have been deposited with the British Library Lending Division as Supplementary Publication No. SUP 35020 (19 pp.). Copies may be obtained through The Executive Secretary, International Union of Crystallography, 5 Abbey Square, Chester CH1 2HU, England.

Table 1. *Positional parameters at* 174 K

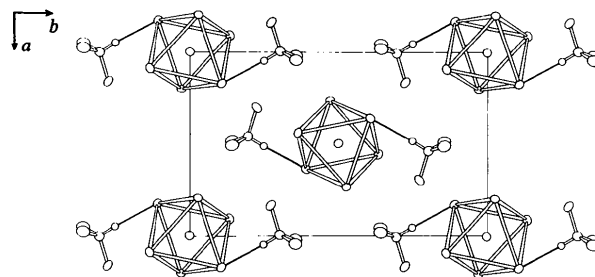|	x	y	z
Cd	0	0	0
Cl(1)	−0·07494 (9)	0·13511 (5)	0·2500
Cl(2)	−0·15588 (8)	−0·10785 (5)	0·2500
Cl(3)	0·21939 (8)	−0·02812 (5)	0·2500
N	0·4789 (3)	0·1961 (2)	0·2500
C(1)	0·3206 (4)	0·2263 (3)	0·2500
C(2)	0·5161 (3)	0·1427 (2)	0·0661 (5)
H(1)	0·532 (4)	0·251 (3)	0·2500
H(2)	0·263 (4)	0·169 (3)	0·2500
H(3)	0·306 (3)	0·261 (2)	0·133 (4)
H(4)	0·449 (3)	0·088 (2)	0·068 (4)
H(5)	0·616 (3)	0·124 (2)	0·072 (4)
H(6)	0·499 (3)	0·181 (3)	−0·043 (5)

Fig. 1. Structure of TrMCd at 174 K. For clarity, the projection along c shows only part of the Cl octahedra. Hydrogen bonds between N and Cl atoms are indicated by single lines.

Table 2. *Bond distances* (Å) *and angles* (°) *for* TrMCd
at 174 K

Cd–Cl(1)	2·6465 (7)	N···Cl(2)ⁱ	3·229 (3)
Cd–Cl(2)	2·6719 (7)	H(1)···Cl(2)ⁱ	2·31 (4)
Cd–Cl(3)	2·6114 (7)		
N–C(1)	1·482 (5)	Cl(1)–Cd–Cl(2)	84·06 (2)
N–C(2)	1·487 (3)	Cl(1)–Cd–Cl(3)	84·24 (2)
N–H(1)	0·92 (5)	Cl(2)–Cd–Cl(3)	84·44 (2)
C(1)–H(2)	0·98 (3)		
C(1)–H(3)	0·94 (3)		
C(2)–H(4)	0·99 (3)	C(1)–N–C(2)	111·4 (2)
C(2)–H(5)	0·93 (3)	C(2)–N–C(2)ⁱⁱ	111·6 (2)

Symmetry code

(i) $\frac{1}{2} - x, \frac{1}{2} + y, z$ (ii) $x, y, \frac{1}{2} - z$.

the type $(NH_3C_nH_{2n+1})_2CdCl_4$ (Chapuis, 1978), indicating a strong hydrogen bond. The anisotropic thermal parameters of the Cd, Cl and N atoms show a quasi-isotropic behavior at 174 K whereas the three C atoms have slightly elongated thermal ellipsoids which can be understood by an oscillation about the local threefold axis containing the N and H atoms of the trimethylammonium ion. This motion has a root-mean-square amplitude of $\sqrt{u_I} = 0·23$ Å, a value much larger than the average perpendicular amplitudes $\sqrt{u_{II}} \simeq \sqrt{u_{III}} = 0·14$ Å.

An interesting feature of this structure is the above-mentioned peak of $0·85$ e Å^{-3} found in the final difference electron density map. This peak is close to the mirror image of the N atom relative to a plane of symmetry through the three C atoms of the trimethyl-ammonium ion. This suggests the existence of a disordered structure where the two configurations represented in Fig. 2 may occur with different probabilities p_1 and p_2 with the condition that $p_1 + p_2 = 1$.

To test the dependence of the probabilities p_i on temperature, the structure of TrMCd was also solved at $T = 295$ K and refined to $R = 0·046$. The analysis revealed that the structures at 174 and 295 K are strictly isomorphous and the difference Fourier synthesis also shows the same residual peak, its height
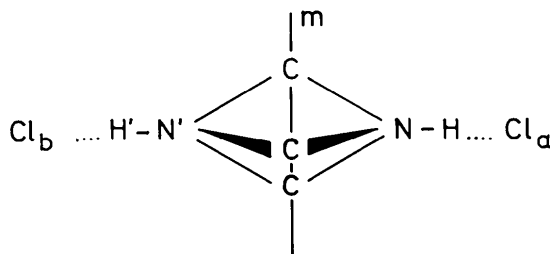
being $1·9$ e Å^{-3} at 295 K ($0·85$ e Å^{-3} at 174 K).[†] It is thus evident that the disorder of the alkylammonium ion increases with temperature and it is to be expected that this should affect the orientation of the CdCl₆ octahedra through the hydrogen bond linking the two entities. The analysis of the thermal motions of the Cl atoms indeed shows that the largest components of their thermal ellipsoids ($\sqrt{u_I} = 0·22$ Å) are always oriented perpendicularly to the Cd–Cl bond and in the ab plane. Such a motion can be accounted for by an oscillation of the octahedra between two equilibrium positions about the pseudo threefold axis parallel to c. A similar increase of the thermal motion affects the three methyl groups. At 295 K, the mean amplitude of the oscillation about the N–H axis is indeed much larger than at 174 K, namely $\sqrt{u_I} = 0·32$ Å. The main difference between the two refinements is thus explained by the amount of disorder of both the CdCl₆ octahedra and the alkylammonium ions.

However, by taking into account the change in the component of the dielectric constant perpendicular to the chain axis at approximately 250 K as observed by Walther (1979), we postulate that the structural disorder observed at 174 K is static whereas the disorder found at room temperature has a dynamical character. Such a hypothesis is also compatible with the changes of the Raman-scattering results observed by Mlik, Daoud & Couzi (1980) in the same domain of temperature. The small enthalpy change found by DTA at 252 K might indicate the activation of the dynamical disorder of the alkylammonium ion as shown in Fig. 2. This disorder then increases continuously up to 342 K.

The existence of disordered N and H atoms has been confirmed independently by the observation of diffuse scattering on Weissenberg diffractograms. This scattering is very weak and concentrated along lines parallel to $\mathbf{a}^* - \mathbf{b}^*$ (or $\mathbf{a}^* + \mathbf{b}^*$). A qualitative interpretation of these lines can be given by considering the structure of TrMCd as a stacking of two different types of layers parallel to the ($\mathbf{a} \pm \mathbf{b}$, $\mathbf{c}$) plane (Fig. 1) with structure factors A_1 and A_2. Each layer type contains parallel chains of CdCl₆ octahedra with their hydrogen-bonded trimethylammonium ions. If n is an integer sequentially characterizing each chain in a layer, layer type A_2 can be generated from A_1 by a rotation of $+60°$ about c for $n = $ even chains and of $-60°$ for $n = $ odd chains. Each type must occur with probabilities p_1 and p_2 respectively to satisfy the average structure obtained from the analysis of the Bragg peaks. The intensity of the diffuse scattering is proportional to $|A_1 - A_2|^2$. This term is small as the only contribution to the difference is given by N atoms. This model explains, therefore, the

Fig. 2. Model of the disordered trimethylammonium ion as found in TrMCd at 174 and 295 K. The mirror plane is locally defined by the three C atoms.

[†] Owing to the similarities between the 174 and 295 K phases, all the relevant crystallographic data, including the atomic coordinates and the list of the observed structure factors for the 295 K phase, have been included in the deposited material only.

weak diffuse intensities observed on the diffracto-
grams.

3. Models for the HHT1 and HHT2 phases

A comparison of the unit-cell constants for the different
phases shows the approximate relations:

$$a_{HHT1} \simeq \tfrac{3}{2}(a^2_{ORT} + b^2_{ORT})^{1/2},$$

$$a_{HHT2} \simeq a_{HHT1}/\sqrt{3},$$

$$c_{ORT} \simeq c_{HHT1} \simeq c_{HHT2}.$$

The unit cells of the three phases of TrMCd represented
in Fig. 3 can all be derived from the hexagonal cell of
the $CsNiCl_3$ structure, also represented in this figure.
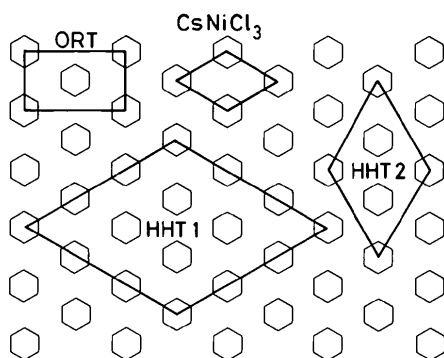The ORT phase of TrMCd approximately satisfies the

Fig. 3. Diagram showing the cells of the TrMCd phases in the ab
plane. The hexagons represent projections of the Cl octahedra
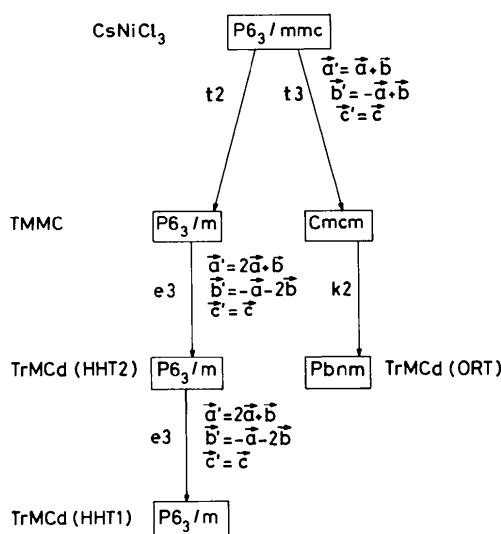along c. For comparison, the $CsNiCl_3$ cell is also shown.

Fig. 4. Diagram of the group–subgroup relations between struc-
tures derived from $CsNiCl_3$. The letters k (same class), t (same
translation) and e (equivalent) followed by the index of the
corresponding subgroup characterize the relation.

condition $\sqrt{3}a_{ORT} \simeq b_{ORT}$ and it can be derived from
$CsNiCl_3$ by replacing Ni by Cd atoms and Cs by
$NH(CH_3)_3^+$. The single-crystal diffraction intensities of
the TrMCd phases support these relationships. In the
ORT phase, the strongest reflections satisfy the
condition $h + k = 2n$, showing that the orthorhombic
structure represents a distortion of a hexagonal
structure with half the unit-cell volume. In the HHT1
phase, all the reflections with $h \neq 3n$ and $k \neq 3n$ are
very weak. This phase is thus a superstructure of the
$CsNiCl_3$ type with the unit-cell volume increased by a
factor of nine. A further increase of the temperature
beyond the next transition shows the disappearance of
part of the weak reflections, yielding a new cell for
HHT2 with a third of the volume of the HHT1 cell.

In both HHT phases of TrMCd, the systematic
absences satisfy the condition $l \neq 2n$ for $00l$. On the
assumption of the presence of a center of symmetry,
the space group $P6_3/m$ is uniquely indicated. The
sequence of phase transitions of TrMCd thus follows
the scheme:

ORT		HHT1		HHT2
	342 K		374 K	
$Pbnm$	⟷	$P6_3/m$	⟶	$P6_3/m$.
$(Z = 4)$		$(Z = 18)$		$(Z = 6)$
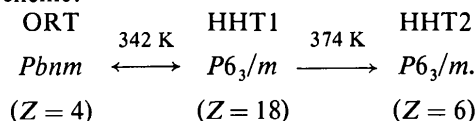
Symmetry arguments thus show that the transition
ORT–HHT1 must be of first order since there is no
group–subgroup relation between the two space groups
(see Fig. 4). Moreover, the first-order character is
obvious from the hysteresis observed by X-ray diffrac-
tion and DTA (Arend, 1979).

The discontinuous shift observed in all the lines on
the powder diffractogram at the HHT1–HHT2 tran-
sition is also characteristic for a first-order phase
transition. This process is, however, irreversible as the
HHT2 lines could still be observed after cooling the
sample to 295 K.

4. Mechanism of the transitions

The comparison of the two structures measured at 174
and 295 K presents useful information on the mecha-
nism of the phase transitions. These two refinements in
space group $Pbnm$ revealed a disorder of the N atoms
which is much larger at room temperature. It is
plausible to assume that the probabilities p_1 and p_2 tend
to be identical with increasing temperature so that
$p_1 = p_2$ at the transition temperature of 342 K. At this
temperature, the disordered model accounts for only
four hydrogen bonds linking the $CdCl_6$ octahedra
instead of the six required by the hexagonal symmetry
of HHT1. A plausible mechanism is to assume the
reorientation of two additional alkylammonium ions
lying in the vicinity of a $CdCl_6$ octahedron to satisfy the
symmetry. This process causes a reordering of the Cl
atoms and introduces a differentiation of adjacent
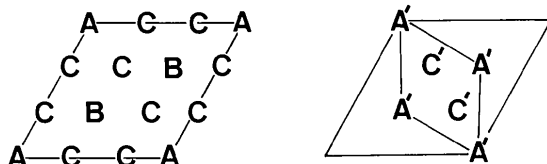octahedra in the same ab plane with respect to their

Fig. 5. Models of the HHT1 (left) and HHT2 (right) cells. Each letter represents Cl octahedra of different point-group symmetry.

hydrogen-bonding schemes. For this reason we observe an increase of the unit cell which is $\frac{9}{2}$ times larger than the ORT cell. The left-hand side of Fig. 5 shows a schematic drawing of the HHT1 structure where the trimethylammonium ions have been omitted. The unit cell contains three different types of $CdCl_6$ octahedra characterized by A, B and C. All A and B octahedra and their associated hydrogen-bonded alkyl-ammonium ions must satisfy the hexagonal symmetry, whereas no conditions are imposed on the C octa-hedra. Both A and B octahedra are surrounded only by C octahedra and are thus completely separated. The structural analysis of the HHT1 phase, which is currently under investigation using single-crystal dif-fraction intensities, confirms this hypothesis.

The model of the HHT1 phase permits an under-standing of the mechanism taking place in the transition at 374 K. The unit cell of HHT2 contains only a third of the atoms found in HHT1 and is obtained by equalizing A and B octahedra as represen-ted on the right-hand side of Fig. 5. The HHT2 cell thus contains only two types of octahedra, A' and C', both with hexagonal symmetry. This transition must be the result of disorder where the A' octahedra result from an averaging of A and B octahedra and their associated alkylammonium ions connected by hydrogen bonds.

The representation in Fig. 4 which is based on the group–subgroup relations of the different phases is of great help for following the transitions. From this diagram, a high-temperature phase with symmetry $P6_3/mmc$ is to be expected. However, such a phase is not obtained because the alkylammonium ion would be required to occupy a special position with point symmetry $\bar{6}m2$, with the N and H atoms located on the mirror plane normal to c. Instead, a new equilibrium is obtained by eliminating part of the alkylammonium ions in the form of [NH(CH₃)₃]Cl. This process necessitates a break-up of some Cd–Cl bonds and causes the major rearrangement of the structure as observed by diffraction. The structure of this phase is still unknown. The final structure obtained beyond 441 K is the layer structure of $CdCl_2$ which results from the total elimination of the alkylammonium ions. If we assume that the rod-like structure exists in [NH(CH₃)₃]Cd₃Cl₇, at least in part, as in [NH(CH₃)₃]₃Mn₂Cl₇ (Caputo, Roberts, Willett & Gerstein, 1976), it is highly probable that the layers of $CdCl_2$ are formed by the juxtaposition of rods

contained in the ac or bc planes of the HHT2 phase. We expect to give a definitive description of this transition mechanism after solving the structure of [NH(CH₃)₃]Cd₃Cl₇.

5. Conclusion

The different phases of TrMCd identified by X-ray diffraction show that the transition mechanisms are induced by the alkylammonium ion linked to a Cl atom by a hydrogen bond. The room-temperature phase revealed the existence of a temperature-dependent disorder of the alkylammonium ion. At the transitions of 341 and 374 K, the ammonium ion behaves such as to avoid the site of hexagonal symmetry observed in TMMC. Instead, we observe two new hexagonal structures with an increase of the cell volume by factors of $\frac{9}{2}$ and $\frac{3}{2}$ respectively, as compared to the room-temperature cell, allowing the ammonium ions to occupy sites with reduced symmetry. Two other phases exist beyond 415 K and result from successive elimination of alkylammonium chloride in the solid state. They were identified as [NH(CH₃)₃]Cd₃Cl₇ and $CdCl_2$ respectively.

References

AREND, H. (1979). Private communication.
BIRGENEAU, R. J. & SHIRANE, G. (1978). Phys. Today, 31, 32–43.
CAPUTO, R. E., ROBERTS, S., WILLETT, R. D. & GERSTEIN, B. C. (1976). Inorg. Chem. 15, 820–823.
CHAPUIS, G. (1978). Acta Cryst. B34, 1506–1512.
CROMER, D. T. & LIBERMAN, D. (1970). J. Chem. Phys. 53, 1891–1898.
CROMER, D. T. & MANN, J. B. (1968). Acta Cryst. A24, 321–324.
MLIK, Y., DAOUD, A. & COUZI, M. (1980). Phys. Status Solidi. Submitted.
MOROSIN, B. & GRAEBER, E. J. (1967). Acta Cryst. 23, 766–770.
SCHWARZENBACH, D. (1977). Abstract PI 20. 4th European Crystallogr. Meet., Oxford.
STEWART, J. M., KRUGER, G. J., AMMON, H. L., DICKINSON, C. & HALL, S. R. (1972). The XRAY system – version of June 1972. Tech. Rep. TR-192. Computer Science Center, Univ. of Maryland, College Park, Maryland.
STEWART, R. F., DAVIDSON, E. R. & SIMPSON, W. T. (1965). J. Chem. Phys. 42, 3175–3187.
WALTHER, U. (1979). Private communication.
WALTHER, U., BRINKMANN, D., CHAPUIS, G. & AREND, H. (1978). Solid State Commun. 27, 901–905.